Major anthocyanins in elderberry effectively trap methylglyoxal and reduce cytotoxicity of methylglyoxal in HepG2 cell line

Sandrine S. Ferreira [a,b], M. Rosário Domingues [c,d], Cristina Barros [c], Sónia A.O. Santos [e], Armando J.D. Silvestre [e], Amélia M. Silva [b,f,*], Fernando M. Nunes [a,g,*]

[a] Chemistry Research Center – Vila Real (CQ-VR), Food and Wine Chemistry Lab., University of Trás-os-Montes and Alto Douro, Quinta de Prados, 5000-801 Vila Real, Portugal
[b] Centre for Research and Technology of Agro-Environmental and Biological Sciences (CITAB-UTAD), University of Trás-os-Montes e Alto Douro, Quinta de Prados, 5001-801 Vila Real, Portugal
[c] Mass Spectrometry Centre, LAQV-REQUIMTE, Department of Chemistry, University of Aveiro, Campus Universitário de Santiago, Aveiro 3810-193, Portugal
[d] CESAM, Centre for Environmental and Marine Studies, Department of Chemistry, University of Aveiro, Campus Universitário de Santiago, Aveiro 3810-193, Portugal
[e] CICECO – Aveiro Institute of Materials, Department of Chemistry, University of Aveiro, 3810-193 Aveiro, Portugal
[f] Department of Biology and Environment, UTAD, 5001-801 Vila Real, Portugal
[g] Department of Chemistry, UTAD, 5001-801 Vila Real, Portugal

ARTICLE INFO

ABSTRACT

The accumulation of advanced glycation end-products (AGEs) in the body is implicated in numerous diseases, being methylglyoxal (MGO) one of the main precursors. One of the strategies to reduce AGEs accumulation might be acting in an early stage of glycation by trapping MGO. Thus, this work aimed to evaluate, for the first time, the potential of elderberries polyphenols to trap MGO, access the formation of MGO adducts, and evaluate the cytoprotection effect in HepG2 and Caco-2 cells. The results demonstrated that monoglycosylated anthocyanins (cyanidin-3-glucoside and cyanidin-3-sambubioside) are very efficient in trapping MGO, forming mono- and di-adducts. Quercetin-3-glucoside and quercetin-3-rutinoside reacted slowly, while diglycosylated anthocyanins did not react. The trapping of MGO by elderberry monoglycosylated anthocyanins significantly decreased the MGO cytotoxicity in HepG2 cells (~70 % of cell viability), while the effect in Caco-2 cells was lower (~50 %). Thus, elderberry phenolics present antiglycation potential by trapping MGO.

1. Introduction

Advanced glycation end-products (AGEs) have gained attention in the last years as the accumulation of AGEs in the body are implicated not only in normal ageing but also in the development of several chronic diseases, like diabetes mellitus and all its associated disorders such as

retinopathy, neuropathy, acceleration of arteriosclerosis and vascular complications (micro- or macrovascular) (G. Chen, 2021; Yeh, Hsia, Lee, & Wu, 2017). AGEs have also been implicated in the development of kidney diseases such as uremia (Henning, Liehr, Girndt, Ulrich, & Glomb, 2014) and have also been associated with neurodegenerative processes such as Alzheimer's and Parkinson's diseases (G. Chen, 2021) and also with cancer cells' growth and metastasis capacity (Nokin, Durieux, Peixoto, Chiavarina, Peulen, Blomme, et al., 2016).

AGEs heterogeneous compounds originate both endogenous and exogenously (G. Chen, 2021; Oliveira, de Almeida, de Souza, da Cruz, & Alfenas, 2021) and are formed mainly from the reaction between the (di) carbonyl groups of reactive electrophilic species and the side chains of amino acid residues of proteins, mainly lysine and arginine (G. Chen, 2021; Yeh, Hsia, Lee, & Wu, 2017). Among the different dicarbonyl compounds, methylglyoxal (MGO), glyoxal (GO), and 3-deoxyglucosone (3-dG), MGO is the most studied as it is one of the most cytotoxic and reactive compounds (Huang, Chuang, Wu, & Yen, 2008). MGO can be produced endogenously and exogenously by enzymatic and non-enzymatic reactions (Maillard reaction) (Yeh, Hsia, Lee, & Wu, 2017). Enzymatic production of MGO, in the organism, is catalysed by methylglyoxal synthase, cytochrome P450 IIE1 isozyme, amine oxidase, triosephosphate isomerase, among other enzymes (Yeh, Hsia, Lee, & Wu, 2017). MGO can also be generated by oxidation of lipids and degradation of triose phosphates and amino acids (Gobert & Glomb, 2009; Yeh, Hsia, Lee, & Wu, 2017). Additionally, intake of exogenous MGO represents another important source. For example, the ingestion of natural plants subjected to severe stress, beverages and food products obtained by fermentation and thermally processed foods that might contain considerable amounts of MGO contribute to human exposure to this compound (Oliveira, de Almeida, de Souza, da Cruz, & Alfenas, 2021; Yeh, Hsia, Lee, & Wu, 2017). MGO is also present in the environment, for instance, in clouds, rainwater or cigarette smoke (Jiang, Huang, Jiao, Bai, Zheng, & Ou, 2019).

The first and most effective antiglycation barrier for MGO and other reactive species in the human body is the glyoxalase system, which detoxifies MGO and other reactive aldehydes. Other strategies include decreasing the formation of Amadori products or Schiff base and of free radicals to reduce dicarbonyl compounds and thus the formation of AGEs (Serin, Akbulut, Uğur, & Yaman, 2021; Yeh, Hsia, Lee, & Wu, 2017). In the last years, several studies, mainly free-cell *in vitro* studies, have confirmed the ability of some phenolic compounds to decrease or inhibit the formation of AGEs, mainly by trapping MGO under physiological conditions. Thus, phenolic compounds can play a significant role in preventing the glycation process and glucose-mediated protein modification. Among the phenolic compounds tested, gallic, vanillic, ferulic and chlorogenic acids (Fernandez-Gomez, Ullate, Picariello, Ferranti, Mesa, & del Castillo, 2015; Silván, Assar, Srey, Dolores del Castillo, & Ames, 2011; Wu, Yeh, Shih, & Yen, 2010), luteolin, rutin, and quercetin (Li, Zheng, Sang, & Lv, 2014; Wu & Yen, 2005), have shown to be effective. Some studies have shown the ability of anthocyanins to trap MGO, namely, delphinidin-3-rutinoside (Chen, Huang, Hwang, Ho, Li, & Lo, 2014), cyanidin-3-rutinoside (Chen, Huang, Hwang, Ho, Li, & Lo, 2014; Thilavech, Ngamukote, Abeywardena, & Adisakwattana, 2015) and cyanidin (Suantawee, Cheng, & Adisakwattana, 2016). The MGO trapping ability by berry compounds, such as blackberry, black raspberry, blueberry, cranberry, red raspberry, and strawberry (Ma, Johnson, Liu, DaSilva, Meschwitz, Dain, et al., 2018) or blackcurrant (Chen, Huang, Hwang, Ho, Li, & Lo, 2014), was demonstrated using *in vitro* free-cell models. However, Jiménez-Aspee, Theoduloz, Ávila, Thomas-Valdés, Mardones, von Baer, et al. (2016) demonstrated that Chilean wild raspberry protected epithelial gastric AGS cells against MGO not by trapping MGO, but by increasing the intracellular levels of reduced glutathione (GSH).

European elderberries (*Sambucus nigra* L.) are one of the richest berries in phenolic compounds (Ferreira, Silva, Silva, & Nunes, 2020). Nevertheless, no study has been performed to evaluate its antiglycation

potential and, to the best of our knowledge, this study is the first to address this question. For this purpose, firstly, we evaluated the potential of elderberry extracts and phenolic standards representative of elderberries' major phenolic components for their capacity to trap MGO. We applied an *in vitro* free-cell model to identify the presence of adducts by direct infusion ESI-MS^n and ultra-high performance liquid chromatography-mass spectrometry (MS). Secondly, we evaluated the antiglycation activity of elderberry extracts, applying cell models, Caco-2 and HepG2 cells, with characteristics and morphology of intestinal epithelium and hepatocytes, respectively, two significant barriers against toxic and xenobiotic agents in the organism.

2. Material and methods

2.1. Samples and preparation of extracts

Elderberries from 'Sabugueiro', 'Sabugueira' and 'Bastardeira' cultivars were used in this study. Elderberries were cultivated in Varosa Valley (Moimenta da Beira, Portugal) and the berries were collected at the commercial ripening stage. Elderberry fruits were exhaustively extracted to obtain all extractable polyphenols, as reported by Ferreira, Silva, Silva, and Nunes (2020). Briefly, 1 g of freeze-dried elderberries were extracted eight times with acidified methanol (1 % HCl). The samples were shaken for 20 min at 200 rpm (Orbital Shaker GFL 3005 series, Hanover, Germany), then centrifuged for 5 min at 10000 rpm (Sigma Centrifuges 3–30 K, St. Louis, MO, USA). The supernatants were collected and pooled, and the final volume was adjusted to 200 mL. The initial extract (E) was further fractioned by SPE using a C18 cartridge (Supelco SPE pack, Sigma-Aldrich), as reported by Ferreira, Silva, and Nunes (2018). After sample application and washing with water (4 × 5 mL), the non-phenolic extract was obtained (H). The retained phenolic compounds were eluted with methanol (4 × 5 mL), yielding the rich-phenolic extract (M). The organic solvent was removed by rotary evaporation (Stuart RE300, Staffordshire, UK), the remaining extract was freeze-dried (Dura DryTM μP) at −41 °C and ~180 mTorr, and chemically characterized as described by Ferreira, Silva, Silva, and Nunes (2020). Furthermore, the phenolic composition of rich phenolic extracts was further characterised by UPLC-MS as described in section 2.4 by comparison of retention time and fragmentation spectra to pure standards (chlorogenic acid, caffeic acid, quercetin, quercetin-3-glucoside, quercetin-3-rutinoside, cyanidin-3-sambubioside, cyanidin-3-glucoside, cyanidin-3-sambubioside-5-glucoside, cyanidin-3,5-diglucoside). For compounds with no phenolic standards available, the fragmentation spectra obtained were compared to those described in the literature.

2.2. Evaluation of MGO trapping capacity by S. nigra extracts under physiological conditions using HLPC-DAD

The *in vitro* free-cell trapping ability of MGO was determined based on experimental conditions described by Gobert and Glomb (2009) and Sang, Shao, Bai, Lo, Yang, and Ho (2007) with some modifications. Briefly, 0.5 mL of MGO (8 mM) and 1.5 mL of different concentrations of elderberry rich-phenolic extracts (0.5, 1 and 2 mg/mL, from 'Sabugueiro', 'Sabugueira' and 'Bastradeira' cultivars) were dissolved in phosphate buffer (pH 7.4, 0.1 M) and incubated at 37 °C for 30 min or 60 min. After the incubation time, acetic acid was added to stop the reaction. Then, to observe possible changes in the profile of phenolic compounds, one set of samples was directly analysed by HPLC-DAD (Ultimate 3000, Dionex) and monitored at 280, 325 and 525 nm, as described by Ferreira, Silva, Silva, and Nunes (2020). The remaining MGO was determined after derivatization using 1,2-phenlyenediamine dihydrochloride (OPD) before HPLC-DAD analysis. For this purpose, after stopping the reaction with acetic acid, 100 μL of OPD was added, and the mixture was incubated for 30 min at 37 °C (Maietta, Colombo, Lavecchia, Sorrenti, Zuorro, & Papetti, 2017). Samples were extracted

three times with dichloromethane (2.5 mL), then evaporated and re-suspended in 1 mL of ethanol:water (1:1) being the amount of methyl-quinoxaline (remaining MGO) analysed by HPLC-DAD. The separation was performed using a reverse-phase C18 column (ACE 5, 250 mm × 4.6 mm, 5 μm; ACE, Scotland) maintained at 35 °C. Being the mobile phase: (A) water and (B) MeOH/water (7:3 (v/v)), and 0.6 mL/L of trifluoroacetic acid was added to both eluents. A flow rate of 1 mL/min was used, and the initial conditions were 80 % (A) during 40 min, changed to 60 % (A) during 15 min, and then the eluent composition was set for the initial conditions. The injection volume was 100 μL, and the remaining MGO was monitored at the same maximum wavelength (317 nm). The decrease in MGO was calculated using the differences of areas before (T0) and after the trapping experiment (T30) and using a calibration curve of MGO (0.5 to 8 mM, y = 106.43x, R^2 = 0.9989).

2.3. Evaluation of MGO trapping capacity by selected phenolic compounds and S. nigra extracts by electrospray ionization mass spectrometry (ESI-MS) analysis

Standard chlorogenic acid, caffeic acid, quercetin, quercetin-3-glucoside, quercetin-3-rutinoside, cyanidin-3-sambubioside, cyanidin-3-glucoside, cyanidin-3-sambubioside-5-glucoside, cyanidin-3,5-diglucoside, and elderberry extracts were analysed by ESI-MS and MS/MS before and after reaction with MGO to characterise the products obtained. The standards and elderberry extracts were dissolved in an appropriate buffer for ESI-MS (ammonium hydrogen carbonate buffer; 5 mM, pH 7.4) at 0.1 mg/mL for standards or at 1 mg/mL for elderberry rich-phenolic extracts. The ESI-MS and MS/MS analyses were performed in a linear ion trap mass spectrometer LXQ (Thermo Finnigan, San Jose, CA). Data acquisition was carried out on a Xcalibur data system as described by Andrea-Silva, Cosme, Ribeiro, Moreira, Malheiro, Coimbra, et al. (2014).

2.4. Evaluation of MGO trapping capacity by selected phenolic compounds by UHPLC-MS analysis

Standard solutions and elderberry extracts, before and after MGO trapping experiments, were analysed by UHPLC-MS (Thermo Scientific Accela HPLC system with an Accela 600 LC pump, Accela 80 Hz Diode-array detector, coupled to an LCQ Fleet ion trap mass spectrometer with an electrospray ionization (ESI) source, ThermoFinniginan, San Jose, CA, USA). A Hypersil GOLD C18 column (100 × 2.1 mm, 1.9 μm, Thermo Fisher Scientific) was used for the analysis with a flow rate of 0.45 mL/min, and the column temperature was maintained at 45 °C. The mobile phase consisted of acetonitrile/water (99:1, v/v) as a mobile phase A and acetonitrile as mobile phase B, both with 0.1 % formic acid. A gradient elution program was applied at a flow rate of 0.45 mL min − 1, as follows: 1 % B kept from 0 to 3 min; 1–31 % B from 3 to 30 min; 31–100 % B from 30 to 32 min, and 100–1 % B from 32 to 36 min, keeping 1 % B from 36 to 40 min for column re-equilibration. A sample volume of 10 μL was injected. Negative and positive modes were used, and the following conditions were applied: spray voltage, 5 V; capillary temperature, 320 °C; capillary voltage, 14/−36 kV (positive/negative); tube lens voltage, 110/−125 V (positive/negative); nitrogen was used as nebulizing and drying gas. Xcalibur data system was used for the data acquisition (Ramos, Moreirinha, Silva, Costa, Veiga, Coscueta, et al., 2019).

2.5. Electron charge calculation

The electron charges for cyanidin, cyanidin-3-*O*-glucoside, cyanidin-3,5-*O*-diglucoside, cyanidin-3-*O*-sambubioside, cyanidin-3-*O*-sambu-bioside-5-*O*-glucoside in the flavylium cation form and carbinol pseudo-base form (hemiketal) and quercetin, quercetin-3-*O*-glucoside, quer-cetin-3-*O*-rutinoside, caffeic acid (dissociated) and 5-chlorogenic acid (dissociated) were calculated using the web-based calculator

AtomicChargeCalculator (Ionescu, Sehnal, Falginella, Pant, Pravda, Bouchal, et al., 2015). AtomicChargeCalculator (ACC) is an application for the calculation and analysis of atomic charges which respond to changes in molecular conformation and chemical environment. ACC relies on an empirical method to compute atomic charges with accuracy comparable to quantum mechanical approaches. The calculation is based on the electronegativity equalization method (Mortier, Ghosh, & Shankar, 1986). ACC is freely available via the Internet at https://ncbr.muni.cz/ACC.

2.6. Cell cultures

Caco-2 (human colon adenocarcinoma, CLS, Eppelheim, Germany) and HepG2 (human hepatoma cell line; ATCC, Rockville, MD, USA) cells were maintained in DMEM (Dulbecco's Modified Eagle Medium) containing 25 mM glucose supplemented with 10 % (v/v) fetal bovine serum (FBS; Gibco, Life technologies), 2 mM L-glutamine (Gibco, Life Technologies), 100 U/mL penicillin (Life Technologies) and 100 μg/mL streptomycin (Life Technologies) at 37 °C in an atmosphere of 5 % CO_2 in air and were handled as described in Ferreira, Silva, and Nunes (2018).

2.7. Evaluation of the effect of elderberry extracts in cell viability

The cytotoxicity of elderberry extract (E), rich-phenolic extract (M), and non-phenolic extract (H) was evaluated in Caco-2 and HepG2 cells. For that, cells were seeded at $5x10^4$ cells/mL onto 96-well microplates and exposed to different concentrations of elderberry extracts (50, 100, 200, 500 and 750 μg/mL), diluted in FBS-free culture medium, for 24 h or 48 h. After the exposure time, cell viability was evaluated by the Alamar Blue assay (Ferreira, Silva, & Nunes, 2018).

2.8. Cytotoxicity assay of MGO

The cytotoxic effects of MGO on cell viability were evaluated by testing ten MGO concentrations (0.5, 1.0, 1.5, 2.0, 2.5, 3.0, 3.5, 4.0, 4.5 and 5.0 mM) for 24 or 48 h of exposure. The assay was repeated on different days, 5-times and 4-times, in Caco-2 and HepG2 cells, respectively. The IC_{50} values were calculated.

2.9. Cytoprotective effect of elderberry extracts against MGO

To evaluate the potential of elderberry extracts in protecting cells against the exposure to MGO (24 h), two assays were conducted: a pre-treatment and a co-treatment. Caco-2 cells were seeded at 5×10^4 cells/mL, then exposed to 12.5, 25, 50 and 200 μg/mL of elderberry extracts for 24 h. After that, the culture media was discarded and replaced by 3 mM MGO for 24 h (diluted in culture medium). Then, cell viability was evaluated by Alamar Blue assay. In the co-incubation treatment the same concentrations were tested, elderberry extract solutions were prepared in FBS-culture medium containing 3 mM MGO, cells were co-incubated for 24 h. The same procedures were performed in HepG2 cells, with the same concentrations of elderberry extracts, but with 2 mM of MGO (as explained in results section).

2.10. Statistical analysis

Chromatographic analyses were performed in duplicate, and cell viability assays were performed in quadruplicate. The data were expressed as mean ± standard deviation (S.D.), and GraphPad Prism software (GraphPad Software Inc., San Diego, CA, USA) was used to perform the statistical analysis (one-way analysis of variance (ANOVA) and Fisher's LSD post-hoc test ($p < 0.05$)).

3. Results and discussion

3.1. Evaluation of S. nigra extracts capacity to trap MGO using HLPC-DAD

The antiglycation potential of elderberry rich-phenolic extracts (M) obtained by SPE was evaluated by measuring their capacity to trap methylglyoxal (MGO). Extracts from the three main Portuguese elderberry cultivars "Sabugueiro", "Sabugueira", and "Bastardeira" harvested at the technological maturity stage were incubated with MGO for 30 min or 60 min. The incubation time of 30 min was selected to perform the trapping assays since this incubation time was enough to reduce near zero the concentration of the major elderberries' anthocyanins in the extracts (Fig. 1a chromatogram at 525 nm). The increased incubation time to 60 min did not increase the reduction of phenolic compounds further than that obtained for 30 min (results not shown). After the incubation time of 30 min, the amount of remaining MGO was measured after reacting with 1,2-phenlyenediamine (OPD), a common trapping agent of dicarbonyl compounds (Gobert & Glomb, 2009) and analysed by HPLC-DAD (Fig. 1b). As shown in Fig. 1b, all the elderberry extracts (from all cultivars) were able to trap MGO. On average, increasing the concentration of elderberry extract allowed to increase MGO consumption, although the increment from 0.5 to 1 mg/mL did not show a significant increase in the consumed MGO. At 2 mg/mL, Sabugueira extract allowed the highest MGO consumption and was significantly higher than Bastardeira, followed by Sabugueiro ($p = 0.0004$ and $p = 0.0100$). While for 0.5 and 1 mg/mL, the MGO consumed was only different between Sabugueira and Bastardeira.

To study if and which polyphenols present in elderberry extracts were the main ones responsible for the observed MGO trapping activity, elderberry extracts were analysed after 30 min reaction with MGO. As can be observed in Fig. 1a and 1c, the main changes were observed on the anthocyanin profile of the extracts (chromatograms at 525 nm), with no significant changes being observed in the cinnamic acids profile (chlorogenic acid) of the extracts (chromatograms at 325 nm). In contrast, for flavonoids, a slight decrease was observed (Fig. 1a, chromatograms at 325 nm). For quercetin-3-glucoside, a minor decrease was observed in all extracts, while for quercetin-3-rutinoside, a decrease was observed at higher concentrations. Cyanidin-3-glucoside and cyanidin-3-sambubioside were almost completely consumed (Fig. 1c), originating several new compounds that appear in the chromatogram at retention times in the 16 to 27 min range and presenting UV–vis spectra different from the original anthocyanins (Fig. 2a). These results show that elderberry monoglycosylated anthocyanins (cyanidin-3-glucoside and cyanidin-3-sambubioside) were responsible for the MGO trapping activity of elderberry extracts, resulting in the formation of several new products, probably MGO adducts. On the other hand, no significant changes in the amount of cyanidin-3,5-diglucoside and cyanidin-3-sambubioside-5-glucoside were observed, suggesting that under the conditions used in this work, diglycosylated anthocyanins do not trap MGO (Fig. 1c). To study if the highest reactivity to trap MGO by monoglycosylated anthocyanins, when compared to the diglycosylated anthocyanins, flavonoids, and cinnamic acids, is due to their lower reactivity in the reaction conditions used or if the results obtained are due to the competition for MGO, as monoglycosylated anthocyanins are in higher concentrations when compared to diglycosylated anthocyanins, flavonoids and cinnamic acids, the MGO trapping capacity of isolated compounds was studied by ESI-MS to evaluate their reactivity and the products formed by the reaction of MGO.

3.2. Evaluation of MGO trapping capacity by selected phenolic compounds using ESI-MS

Nine phenolic compounds, seven occurring in elderberry extract, including cinnamic acid derivatives (chlorogenic and caffeic acids), flavonols (quercetin, quercetin-3-glucoside, and quercetin-3-rutinoside) and anthocyanins (cyanidin-3-sambubioside, cyanidin-3-glucoside, cyanidin-3-sambubioside-5-glucoside and cyanidin-3,5-diglucoside) were analysed by ESI-MS before and after reacting with MGO, in positive and negative ion mode for all the standards. However, here we present only the data obtained in positive ion mode for anthocyanins and negative ion mode for the other phenolic compounds, summarized in Table S1. The ESI-MS^2 spectra obtained are shown in Figs. 3-4. At acidic pH, anthocyanins have a positive charge, thus ionizing preferentially in positive ion mode as M$^+$ ions. In contrast, cinnamic derivatives and flavonols ionize preferentially with the formation of negatively charged ions [M – H]$^-$.

The MS^2 spectra of the main anthocyanin standards from elderberry are shown in Fig. 2 (Chen, Huang, Hwang, Ho, Li, & Lo, 2014), namely cyanidin-3-glucoside (M$^+$ ion at $m/z = 449$), cyanidin-3-sambubioside (M$^+$ ion at $m/z = 581$), cyanidin-3,5-diglucoside (M$^+$ ion at $m/z = 611$) and cyanidin-3-sambubioside-5-glucoside (M$^+$ ion at $m/z = 743$). The main product ions observed for these anthocyanins correspond to the cyanidin aglycone ($m/z = 287$), resulting from the loss of the sugar substituents in the O-3 position for cyanidin-3-glucoside (–162 Da, –Glc) and cyanidin-3-sambubioside (–294 Da, –XylGlc) and the sequential loss of the sugars from O-3 and O-5 positions for cyanidin-3,5-diglucoside (–162 Da, –162 Da; –Glc, –Glc) and cyanidin-3-sambubioside-5-glucoside (–162 Da, –294 Da; –Glc, –XylGlc). When these anthocyanins were incubated with MGO, no adducts were formed for cyanidin-3,5-diglucoside and cyanidin-3-sambubioside-5-glucoside. At the same time, new compounds were identified corresponding to the mono- and di-MGO adducts of cyanidin-3-glucoside and cyanidin-3-sambubioside. The addition of one or two MGO molecules to anthocyanins can easily be inferred by the presence of the M$^+$ ions at m/z 521 and 593 for the mono- and di-MGO adduct of cyanidin-3-glucoside and ions at m/z 653 and 725 for the mono- and di-MGO adduct of cyanidin-3-sambubioside, respectively. The MS^2 spectra of these newly formed compounds further support the presence of one or two MGO adducts. For the mono-MGO adduct of cyanidin-3-glucoside, the MS^2 spectrum showed a product ion at m/z 503 due to the loss of one water molecule (–H$_2$O) and a product ion at m/z 449 was formed due to the loss of one methylglyoxal molecule (–72 Da). The loss of the glucose moiety (–162 Da) renders the product ion [M – Glc]$^+$ at m/z 359 which corresponds to the MGO adduct of cyanidin (287 Da + 72 Da). The product ions at m/z 341 and 287 correspond to the loss of one water molecule and one MGO molecule from ion at m/z 359 [M – Glc]$^+$. The same fragmentation profile was reported for the mono-MGO adduct of the cyanidin-rutinoside and mono-delphinidin-3-rutinoside adduct with MGO (Chen, Huang, Hwang, Ho, Li, & Lo, 2014). For the di-MGO adduct of cyanidin-3-glucoside (M$^+$ at $m/z = 593$), the same fragmentation pattern is observed in the MS^2 spectrum. The product ions at m/z 525 and 557 are attributed to the loss of one and two water molecules, respectively. The product ions at m/z 521 and 503 are attributed to the loss of one MGO molecule and the combined loss of one water molecule and one MGO molecule, respectively. The ion at m/z 431 was attributed to the di-MGO-cyanidin aglycone, and the ions at m/z 413, 395, 359 and 341 were attributed to the loss of one, two water molecules plus one MGO molecule, respectively. The same fragmentation pattern was observed in the MS^2 spectra obtained for the mono-MGO (M$^+$ at $m/z = 653$) and di-MGO derivatives (M$^+$ at $m/z = 725$) cyanidin-3-sambubioside, also confirming the formation of MGO adducts for cyanidin-3-sambubioside. These results are in accordance with the results obtained by HPLC-DAD, confirming the reactivity of cyanidin-3-glucoside and cyanidin-3-sambubioside with MGO and the lack of reactivity of cyanidin-3,5-diglucoside and cyanidin-3-sambubioside-5-glucoside under the conditions used in this work. Several studies conducted by UHPLC-MS and NMR proved that the major active site of polyphenols to trap reactive dicarbonyl compounds, as MGO, is linked to the A-ring, more specifically, for flavonoids in the position C8 for mono-adducts, and C8 and C6 for the di-adducts (Hwang, Kim, Zuo, Wang, Lee, & Lim, 2018; Lv, Shao, Chen, Ho, & Sang, 2011; Sang, Shao, Bai, Lo, Yang, & Ho, 2007). The
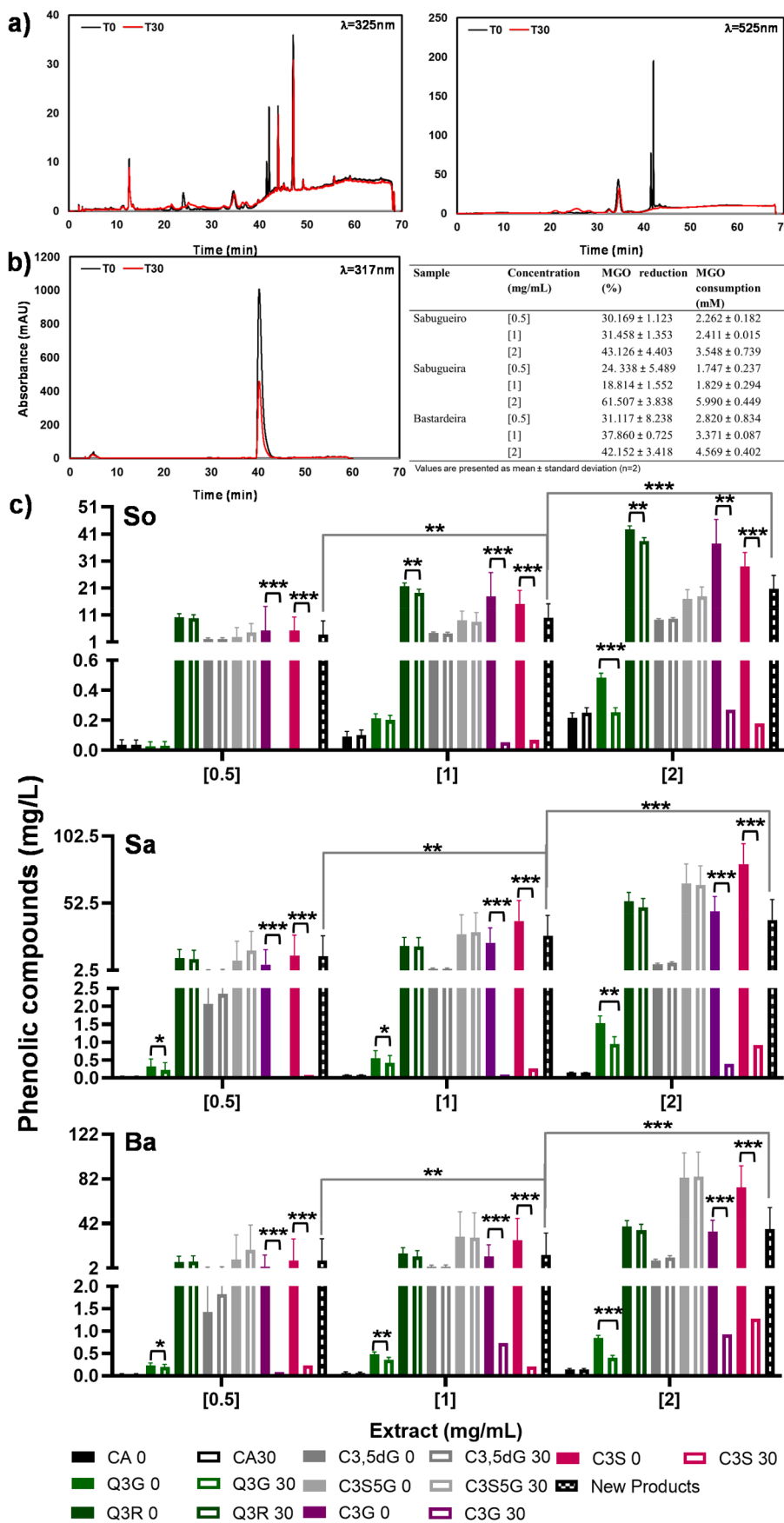
Fig. 1. (a) Effect of rich-phenolic elderberry extracts at 1 mg/mL and its changes in the polyphenol profile, assessed by HPLC-DAD, before (T0) and (T30) after the trapping experiment, under physiological conditions; (b) Reduction of methylquinoxaline detected at 317 nm after the trapping experiment in rich-phenolic elderberry extracts (left) and effect of extracts concentration on MGO reduction and consumption (right); (c) Concentration of the major phenolic compounds of rich-phenolic elderberries extracts (So, Sa and Ba cultivars) before and after the trapping experiment and the formation of new products (confidence levels: *: $p < 0.05$; **: $p < 0.001$ and ***:$p < 0.0001$).
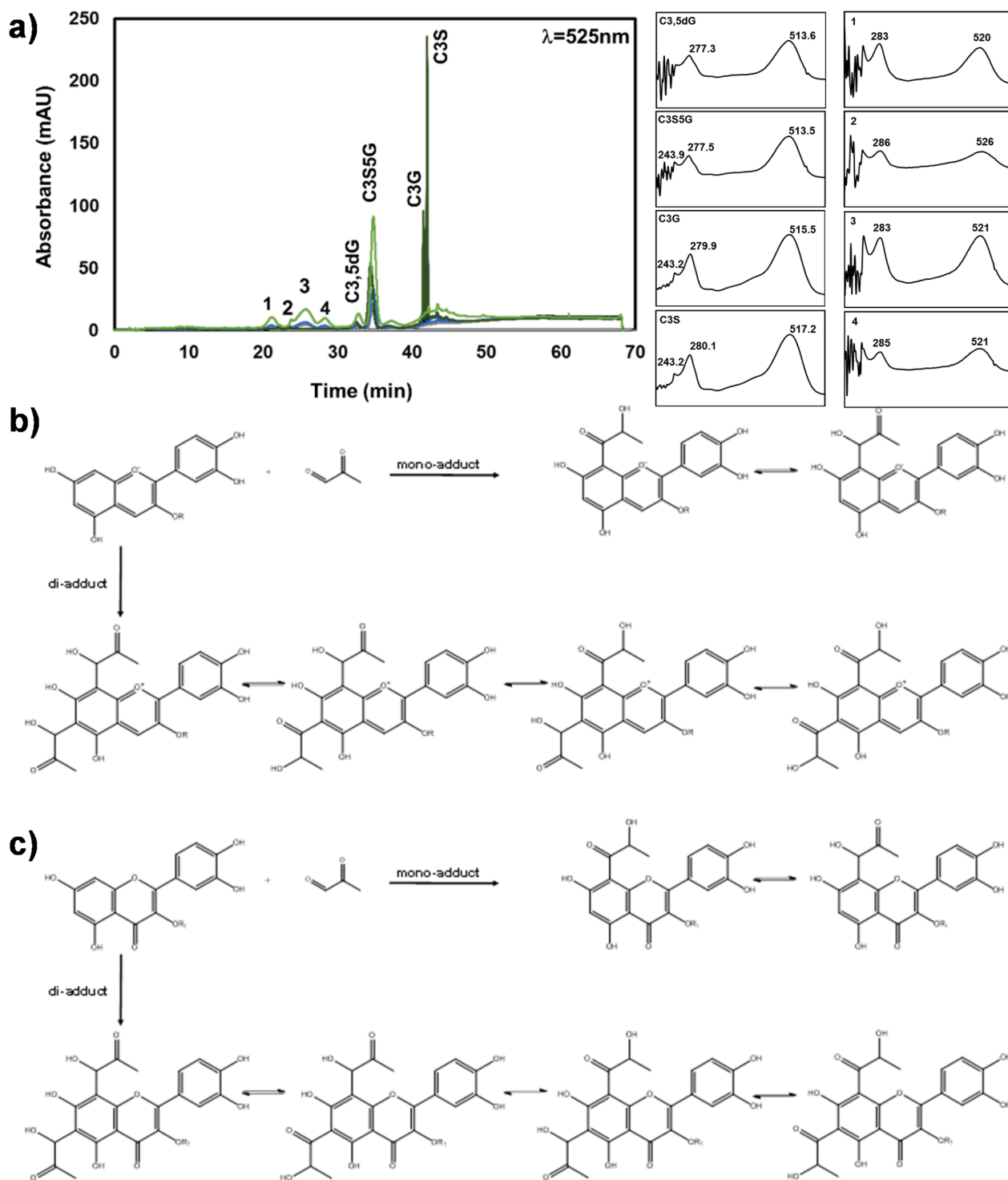
Sample	Concentration (mg/mL)	MGO reduction (%)	MGO consumption (mM)
Sabugueiro	[0.5]	30.169 ± 1.123	2.262 ± 0.182
	[1]	31.458 ± 1.353	2.411 ± 0.015
	[2]	43.126 ± 4.403	3.548 ± 0.739
Sabugueira	[0.5]	24. 338 ± 5.489	1.747 ± 0.237
	[1]	18.814 ± 1.552	1.829 ± 0.294
	[2]	61.507 ± 3.838	5.990 ± 0.449
Bastardeira	[0.5]	31.117 ± 8.238	2.820 ± 0.834
	[1]	37.860 ± 0.725	3.371 ± 0.087
	[2]	42.152 ± 3.418	4.569 ± 0.402

Values are presented as mean ± standard deviation (n=2)

Fig. 2. (a) Changes in the anthocyanin profile of rich-phenolic elderberry extracts (0.5, 1 and 2 mg/mL) before and after the trapping experiment (left), and UV–vis spectra of the new products formed (right); (b) Proposed reaction pathways of mono- and di-MGO adducts formation between cyanidin-3-glucoside and cyanidin-3-sambubioside and methylglyoxal (R: glucose or sambubiose moiety); (c) Proposed reaction pathways of mono- and di-MGO adducts formation between quercetin-3-glucoside and quercetin-3-rutinoside (R1: glucose or rutinose moiety).

glucose residue in position C5 of A-ring might explain this lack of reactivity of anthocyanins (Shao, Bai, He, Ho, Yang, & Sang, 2008). The atomic charge of anthocyanin carbons was calculated to evaluate the effect of glucose at the C5 position, and results are presented in Figs. S5 and S6 (Supplementary material). Linkage of a glucose residue at the C5 position (A-ring) did not change the atomic charge of cyanidin-3,5-diglucoside significantly compared to cyanidin-3-glucoside and

cyanidin-3-sambubioside-5-glucoside, when compared to cyanidin-3-sambubioside in the carbinol pseudo base form. In fact, at the reaction conditions used for trapping MGO (pH = 7.4), the carbinol pseudo base is the main form of anthocyanins present in the solution (Andrea-Silva, et al., 2014). Thus, the adduct formation of anthocyanins with MGO occurs in this form. Therefore, steric hindrance seems to be a decisive factor in MGO nucleophilic substitution reaction in anthocyanins
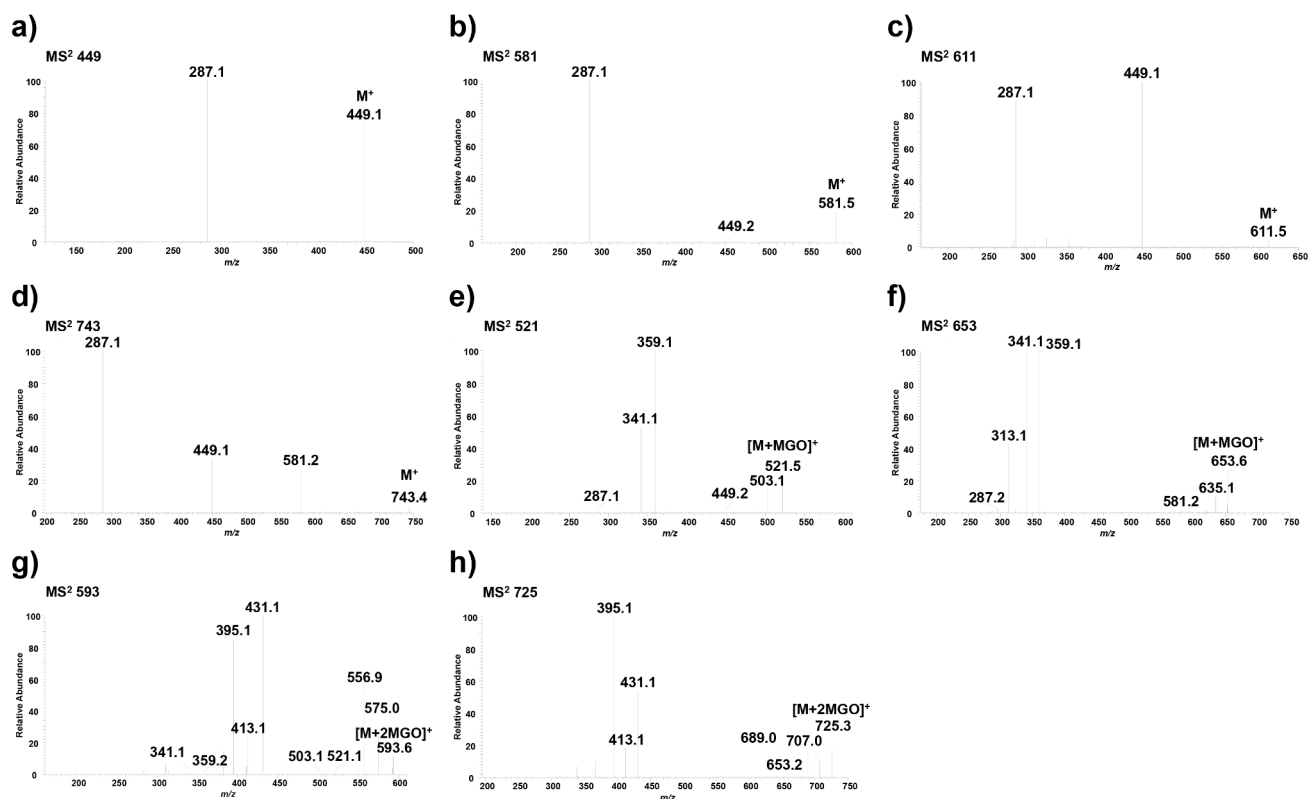
Fig. 3. ESI-MS^2 spectra of anthocyanin standards identified by ESI-MS as [M]$^+$: before the trapping experiment: (a) cyanidin-3-glucoside; (b) cyanidin-3-sambubioside; (c) cyanidin-3,5-diglucoside and (d) cyanidin-3-sambubioside-5-glucoside; as well as the formation of mono-methylglyoxal (MGO) adduct of (e) cyanidin-3-glucoside and of (f) cyanidin-3-sambubioside and formation of di-MGO adducts of (g) cyanidin-3-glucoside and of (h) cyanidin-3-sambubioside after the trapping experiment.

substituted at C5 (Chen, Huang, Hwang, Ho, Li, & Lo, 2014). Results reported by Shao, Bai, He, Ho, Yang, and Sang (2008) support this assumption, demonstrating that the aglycone phloretin had a higher ability to trap MGO than phloridzin. The glycosylation in A-ring for phloridzin (which occurs in the same position in cyanidin-3,5-diglucoside and cyanidin-3-sambubioside-5-glucoside) considerably slows down the trapping ability taking more time to react and form adducts.

Fig. 3, shows the negative ion MS^2 spectra of the main flavonol standards well know from elderberry (Fabre, Rustan, de Hoffmann, & Quetin-Leclercq, 2001), namely quercetin-3-glucoside ([M – H]$^-$ at m/z = 463), quercetin-3-rutinoside ([M – H]$^-$ at m/z = 609) and quercetin ([M – H]$^-$ at m/z = 301). As observed for O-3 substituted anthocyanins, these O-3 substituted flavonols also showed the formation of mono- and di-MGO adducts when incubated with MGO at the conditions used in this work and inferred by the observation of new ions in the ESI-MS spectra. On the other hand, quercetin was not able to react with MGO under the same conditions. Table S2 displays the most characteristic product ions observed for each compound obtained after analysing the corresponding MS^2 spectra from the [M − H]$^-$ ions. Product ions, except retrocyclization ions, observed in the MS^2 spectra were noted by the corresponding aglycone number followed by an alphabetical letter in the order of the increasing mass to charge ratio. The nomenclature adopted for the retro Diels-Alder (RDA) cleavages was adapted from the one proposed by Brüll, Heerma, Thomas-Oates, Haverkamp, Kovácik, and Kovác (1997) and Domon and Costello (1988). Fig. S1 shows the various retrocyclization product ions observed in this study. These fragments can undergo further fragmentation, as denoted in Table S2. The fragmentation observed in the MS^2 spectrum of quercetin ([M – H] $^-$ at m/z = 301) shows the typical product ions resulting from the losses of CO (m/z = 273) and CO_2 (m/z = 257) and the consecutive losses of CO_2 and CO (m/z = 229). The product ion at m/z 193 is attributed to the B-ring

loss, and the base product ion at m/z 179 (the base peak of the MS^2 spectrum) is attributed to retrocyclisation yielding the product ion ^{1,2}A$^-$. The consecutive loss of CO from the product ion yield at m/z 179 yields the product ion at m/z 151. Product ions at m/z 121 and 107 are also attributed to retrocyclisation yielding the ^{1,2}B$^-$ ion and the consecutive loss of CO and CO_2 from ^{1,2}A$^-$ ion. Incubation of quercetin under the reaction conditions did not result in the formation of MGO-adducts. Products resulting from the incubation of quercetin-3-glucoside and quercetin-3-rutinoside with MGO resulted in the formation of [M – H]$^-$ ions at m/z 535 and m/z 607 for quercetin-3-glucoside and ions m/z 681 and m/z 753 for quercetin-3-rutinoside that were attributed to the formation of mono- and di-MGO adducts of quercetin-3-glucoside and quercetin-3-rutinoside, respectively. The formation of mono- and di-MGO adducts can be inferred from the MS^2 spectra of the newly formed compounds (Fig. 3 and Table S2). The loss of glucose and rutinoside residues from [M – H]$^-$ ions at m/z 535 and m/z 681, respectively, a mono-MGO adduct of quercetin-3-glucoside and quercetin-3-rutinoside, yielded the product ion at m/z 373 that was attributed to MGO adduct of the aglycone quercetin. The same rationale is observed for the MS^2 spectra of [M – H]$^-$ ions at m/z 607 and m/z 753 (di-MGO adducts of quercetin-3-glucoside and quercetin-3-rutinoside) that show the product ion at m/z 445 formed by loss of a glucose or rutinoside residues, respectively. The product ion at m/z 445 observed in both MS^2 spectra was attributed to di-MGO adduct of quercetin. The presence of product ions at m/z 251 for mono-MGO adduct of quercetin-3-glucoside and quercetin-3-rutinoside, attributed to ion ^{1,2}A$^-$ after losing the sugar residues, confirms that the substitution occurs in the A-ring of quercetin. Also, product ions at m/z 295 and m/z 277 in MS^2 spectrum of ion at m/z 607, attributed to ^{1,2}A$^-$ – CO and ^{1,2}A$^-$ – CO – H_2O ions, confirms that di-substitution of quercetin-3-glucoside by MGO also occur in the A-ring of quercetin.

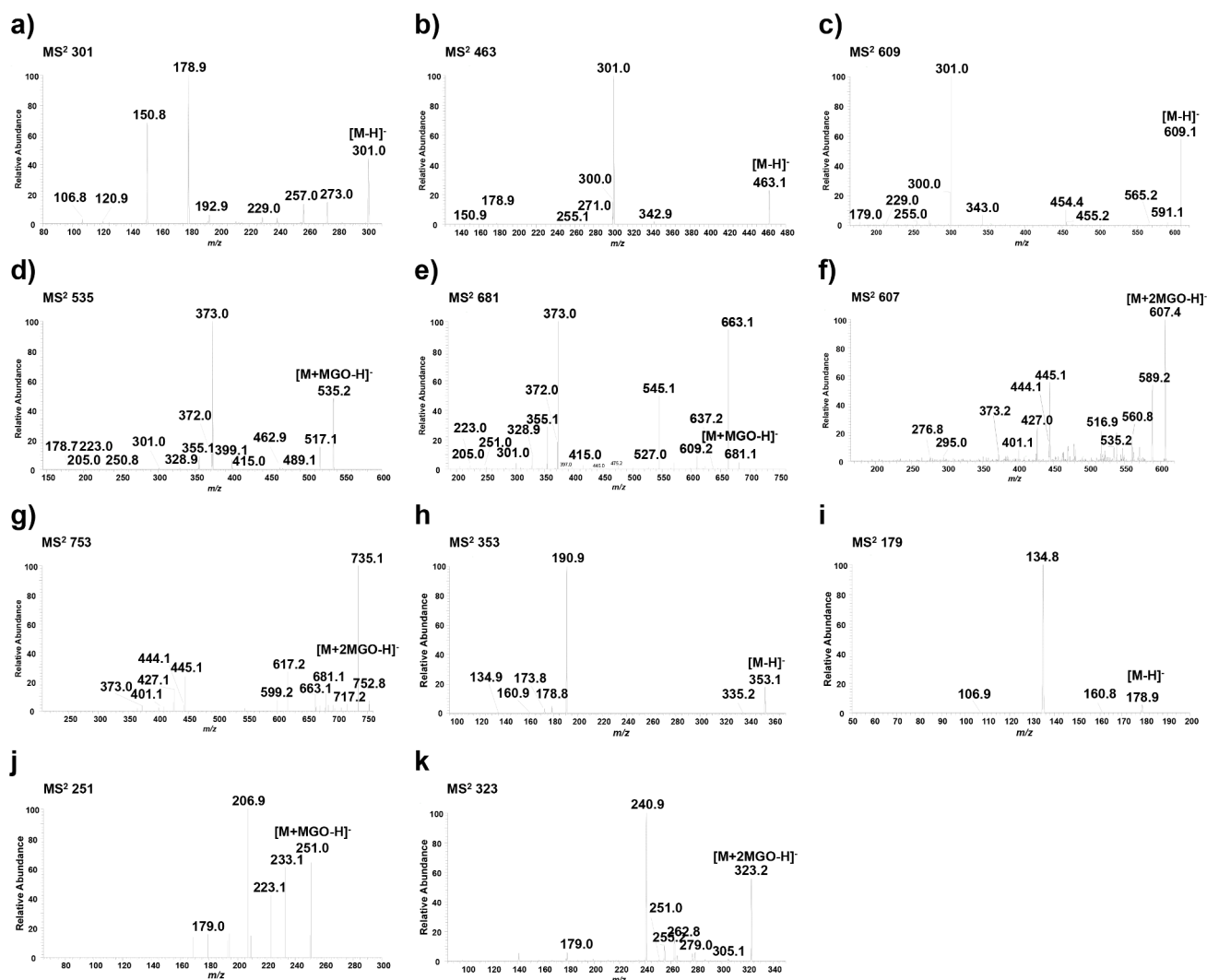Based on the present results and the literature (Hwang, Kim, Zuo,

Fig. 4. ESI-MS^2 spectra of flavonol standards identified by ESI-MS as [M−H]⁻: before the trapping experiment: (a) quercetin; (b) quercetin-3-glucoside; (c) quercetin-3-rutinoside as well as the formation of mono-methylglyoxal (MGO) adduct of (d) quercetin-3-glucoside and (e) quercetin-3-rutinoside and formation of di-MGO adducts of (f) quercetin-3-glucoside and of (g) quercetin-3-rutinoside after the trapping experiment. ESI-MS^2 spectra of (h) chlorogenic acid (i) and caffeic acid before the trapping experiment, as well as the formation of mono-methylglyoxal (MGO) adduct of (j) caffeic acid and formation of di-MGO adducts of (k) caffeic acid after the trapping experiment.

Wang, Lee, & Lim, 2018; Lv, Shao, Chen, Ho, & Sang, 2011; Sang, Shao, Bai, Lo, Yang, & Ho, 2007), Fig. 1e shows the proposed reaction pathways of cyanidin-3-glucoside and cyanidin-3-sambubioside mono- and di-adducts formation. Fig. 1f shows the proposed reaction pathways of quercetin-3-glucoside and quercetin-3-rutinoside.

Under the experimental conditions used in this work, chlorogenic acid (Fig. 4a) did not show the formation of mono- and di-MGO adducts. MS^2 spectrum of [M – H]⁻ ions (m/z 353) obtained for chlorogenic acid is in accordance with the literature, being observed the product ions at m/z 191 (Q1 [quinic acid – H]), m/z 179 (C1 [caffeic acid – H]), m/z 173 (Q2 [quinic acid – H$_2$O]), and at m/z 135 (C2 [caffeic acid – CO$_2$] (Jaiswal, Halabi, Karar, & Kuhnert, 2014). However, some studies have shown the ability of chlorogenic acid to trap and inhibit MGO action (Fernandez-Gomez, Ullate, Picariello, Ferranti, Mesa, & del Castillo, 2015). This difference in reaction outcome can be explained by the reaction conditions (lower reaction time and concentration used in our work). Also, Li, Zheng, Sang, and Lv (2014) demonstrated that quercetin could trap MGO forming mono- and di-adducts, depending on the concentration and incubation time. To understand if the lack of reactivity of chlorogenic acid can be due to the lack of reactivity of the phenolic moiety of this molecule, caffeic acid was incubated with MGO under the same

conditions as chlorogenic acid. Caffeic acid ([M – H]⁻ ion at m/z 179, Fig. 4b)) showed the typical product ions formed due to CO$_2$ elimination yielding product ion at m/z 135 and consecutive loss of CO yielding a product ion at m/z 107. The loss of H$_2$O generates the product ion at m/z 161 (Jaiswal, Halabi, Karar, & Kuhnert, 2014). The incubation of caffeic acid with MGO resulted in two compounds corresponding to negative ions at m/z 251 and 323 that were attributed to the formation of mono- and di-MGO adducts of caffeic acid. MS^2 spectrum of caffeic acid mono-MGO adduct (Fig. 4c) shows the same fragmentation pattern of unsubstituted caffeic acid, showing the loss of CO$_2$ yielding the product ion at m/z 207, but also the loss of H$_2$O yielding the ion at m/z 233 and the loss of CO yielding the ion at m/z 233. Also observed is the product ion at m/z 179 resulting from the loss of MGO (–72 Da). For di-caffeic acid-MGO adduct (m/z 323, Fig. 4d), the loss of CO$_2$ (m/z 279), H$_2$O (m/z 305) and the consecutive losses of H$_2$O plus H$_2$CO$_2$ (m/z 241) are observed. Also observed are the successive losses of one MGO residue (m/z 251) and two MGO residues (m/z 179). Therefore, under the incubation conditions used in this work, caffeic acid could form mono- and di-MGO adducts, but its reactivity decreased when esterified with quinic acid.

3.3. Evaluation of MGO trapping capacity by selected phenolic compounds by UHPLC-MS analysis

The reaction products obtained by reaction of selected phenolic compounds and *S. nigra* extracts with MGO were further analysed by UHPLC-MS to confirm the results obtained by direct injection ESI-MS (Fig. 5), as it can decrease eventual matrix suppression effects and detect possible isomeric structures (Pitt, 2009).

The profile of anthocyanin standards before the trapping experiment is shown in Fig. 5a, and the profile obtained after the trapping experiment is shown in Fig. 5b, c, d and e. The obtained results showed that cyanidin-3,5-diglucoside (Fig. 5b) and cyanidin-3-sambubioside-5-glucoside (Fig. 5c) did not demonstrate ability to trap MGO, being present only one compound at 8.31 and 10.30 min, respectively, corresponding to the respective native anthocyanins (Fig. 2c and 2d, respectively). On the other hand, after MGO trapping, cyanidin-3-glucoside (Fig. 5d) showed the formation of two new compounds, at 8.98 min ($m/z = 593$) corresponding to di-MGO adduct and at 11.25 min ($m/z = 521$) corresponding to mono-MGO adduct, presenting the same MS^2 mass spectrum as those obtained by direct injection ESI-MS (Fig. 2e and g). In contrast, cyanidin-3-glucoside (17.16 min) was almost totally consumed. Regarding cyanidin-3-sambubioside (Fig. 5e), after the MGO trapping experiment, this anthocyanin was also consumed (no peak found at 18.07 min), and two new compounds were formed at 10.91 min ($m/z = 725$; di-adduct) and 13.99 min ($m/z = 653$; mono-adduct).

Concerning the other phenolic compounds, commercial standards of chlorogenic acid, quercetin-3-glucoside and quercetin-3-rutinoside were also analysed by UHLC-MS, before (Fig. 5f, mix of all standards) and after MGO trapping (Fig. 5g, h and i, respectively). Results confirmed that in our experimental conditions, chlorogenic acid did not show the ability to trap MGO (Fig. 5g). As shown in Fig. 5h and 5i, the amount of unreacted quercetin-3-glucoside and quercetin-3-rutinoside remains very high after the MGO trapping experiments being detected only the formation of mono-adducts for both quercetins.

3.4. Evaluation of MGO trapping capacity by S. nigra extracts by electrospray ionization mass spectrometry (ESI-MS) and MS/MS analysis

To confirm the formation of mono- and di-MGO adducts of the studied phenolic compounds when elderberry extracts are incubated with MGO, elderberries samples (1 mg/mL) were analysed by ESI-MS in negative and positive ion mode (Fig. S2) before and after incubation with MGO. Chlorogenic acid, quercetin, quercetin-3-glucoside, quercetin-3-rutinoside, cyanidin-3-glucoside, cyanidin-3-sambubioside, cyanidin-3,5-diglucoside and cyanidin-3-sambubioside-5-glucoside were identified both in negative and positive mode (Fig. S2a and b, respectively) before incubation with MGO. However, quercetin-3-rutinoside was only detected in negative ion mode, and cyanidin-3,5-diglucoside was only detected in positive ion mode. After MGO trapping experiment, although the initial phenolic compounds detected in the extracts were still present, it was also possible to observe the new ions corresponding to the formation of mono- and di-MGO adducts of some of them (Fig. S3-S4). The data showed clearly the formation of both mono- and di-adducts for cyanidin-3-glucoside, cyanidin-3-sambubioside, quercetin-3-glucoside, and quercetin-3-rutinoside. The ESI-MS^2 and MS/MS fragmentation were identical to the fragmentation when using isolated standards (Figs. 2-4).

When comparing the full ESI-MS in negative ion mode obtained for the sample before (Fig. S2 a) and after trapping (Fig. S2 c), it is clear that the molecular ion at m/z 609 ([M − H]$^−$ of quercetin-3-rutinoside) presented the highest relative abundance before and after the trapping experiment, which might indicate in these experimental conditions, that quercetin-3-rutinoside reacted slowly or/and poorly reacted with MGO, when compared with the anthocyanins present in elderberry extracts. Moreover, the ion of quercetin-3-glucoside (m/z 463, [M − H]$^−$) also showed a considerable relative abundance after the trapping

experiment. Combining all this information and considering the initial profile obtained by HPLC-DAD (Fig. 1), it can be inferred that quercetin derivatives were less efficient in trapping MGO when compared to anthocyanins (Fig. 1).

Wu and Yen (2005) demonstrated that the potential of phenolic compounds to prevent or inhibit AGEs formation depends on the stage of glycation, such as the early, middle and last stages using different BSA (bovine serum albumin) models. Ten phenolic compounds were tested (catechin, epicatechin, epicatechin gallate, epigallocatechin, epigallocatechin gallate, kaempferol, luteolin, quercetin, naringenin and rutin), luteolin, quercetin, and rutin, all exhibited a significant inhibitory effect in the early stage of glycation. In the middle stage of glycation, the more effective compounds were luteolin and rutin, and in the last stage of glycation, only luteolin inhibits AGEs formation. Gugliucci, Bastos, Schulze, and Souza (2009) demonstrated that caffeic acid, chlorogenic acid and oleanolic acid, to a lesser extent, presented anti-glycation potential inhibiting the AGEs fluorescence by applying two different proteins models (bovine serum albumin and histones). Fernandez-Gomez, Ullate, Picariello, Ferranti, Mesa, and del Castillo (2015) also demonstrated that chlorogenic acid inhibited the formation of AGEs using a BSA model. Other phenolic compounds as ferulic acid (Silván, Assar, Srey, Dolores del Castillo, & Ames, 2011) and cyanidin-3-rutinoside (Thilavech, Ngamukote, Abeywardena, & Adisakwattana, 2015) also presented anti-glycation potential and attenuated the AGEs formation using different protein-models.

3.5. Cytoprotective effect of elderberry extracts against MGO

Considering the results obtained using the *in vitro* free-cell model, we evaluate the potential protective effect of elderberry extracts using Caco-2 and HepG2 cells. To select non-cytotoxic concentrations of elderberry extracts and cytotoxic concentrations of MGO (IC$_{50}$), the exposure of cells to elderberry extracts (50 – 750 µg/mL) was first evaluated for 24 h and 48 h incubations in both cell lines. All extracts, at all tested concentrations, did not show to be cytotoxic (data not shown). The cytotoxic effect of different concentrations of MGO (0 – 5.0 mM) was evaluated for 24 h and 48 h exposure, as shown in Fig. 6a. Results obtained in Caco-2 cells for 24 h of exposure (Fig. 6a1) showed an IC$_{50}$ = 3.06 ± 0.05 mM, however concentrations between 0.5 and 2 mM were not cytotoxic (cell viability ∼ 100 % of untreated control) but higher doses of MGO dose-dependently reduces cell viability (Fig. 6a1). Moreover, 48 h exposure of Caco-2 cells to MGO increased the cytotoxicity, as the IC$_{50}$ decreased to 2.66 ± 0.03 mM. However, 0.5, 1 and 1.5 mM MGO, for 48 h exposure, did not affect Caco-2 cell viability being the percentage of viable cells ∼ 100 % of untreated control ($p <$ 0.05) (Fig. 6a1), but, cell morphology presents small changes (Fig. 6a2). Concentrations higher than 2 mM dose-dependently reduce cell viability (Fig. 6a1; grey bars), alter cell morphology, and reduce the number of cells per well (Fig. 6a2).

The effect of MGO on HepG2 cells viability after 24 h exposure is shown in Fig. 6a3 (black bars) and is also dose-dependent, with an IC$_{50}$ of 2.12 ± 0.05 mM. At higher concentrations, i.e. 4, 4.5 and 5 mM, high cytotoxic effect is observed, being cell viability only ∼ 1 % of control. For 48 h exposure, an IC$_{50}$ of 1.95 ± 0.03 mM was obtained. Fig. 6a4 shows the morphology of HepG2 cells exposed to different concentrations of MGO, as depicted. As these cells grow in small aggregates, it is more challenging to observe morphological changes, however, the reduced number of cells at higher MGO concentrations is noticeable (Fig. 6a4).

These results show the high cytotoxicity of MGO to both cell lines, being HepG2 cells more sensitive than Caco-2 cells, based on the IC$_{50}$ values. Thus, next, we evaluated the potential protective effect of elderberries against MGO-induced injuries in cells incubated with MGO (at ∼ IC$_{50}$) for a period of 24 h by using a pre-incubation with elderberry extracts before exposure to high doses of MGO, as well as a co-incubation of the cells with elderberry extracts and MGO for 24 h
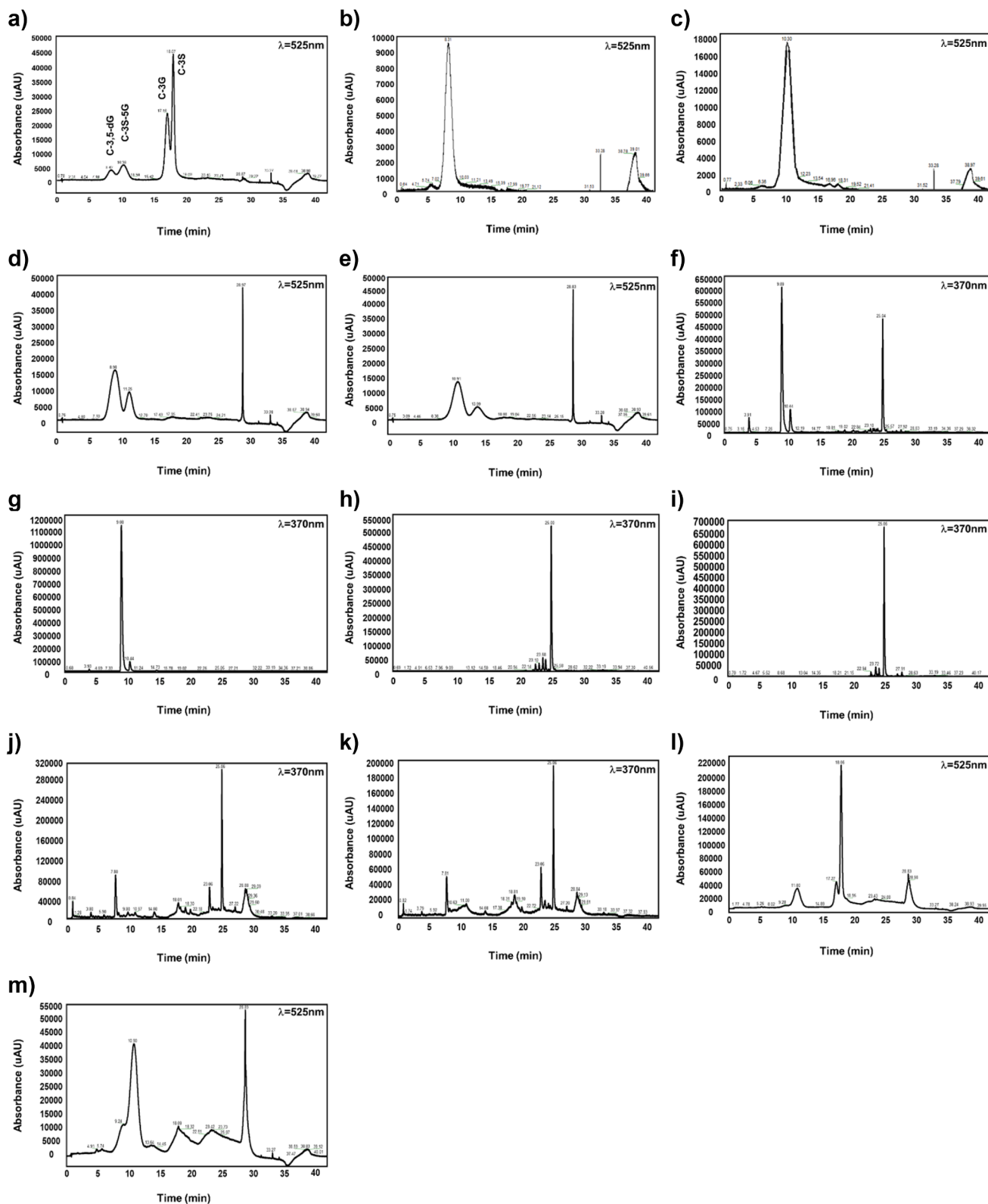
Fig. 5. Chromatograms obtained by UHPLC-MS of each standard and of samples before (T0) and after (T30) the trapping experiment. a) anthocyanins mix (T0); b) cyanidin-3,5-diglucoside (T30); c) cyanidin-3-sambubioside-5-glucoside (T30); d) cyanidin-3-glucoside (T30); e) cyanidin-3-sambubioside (T30); f) phenolic compounds mix (T0); g) chlorogenic acid (T30); h) quercetin-3-glucoside (T30) and i) quercetin-3-rutinoside (T30); j) phenolic elderberries sample (T0); k) phenolic elderberries sample (T30); l) anthocyanin elderberries sample (T0) and m) anthocyanin elderberries sample (T30).
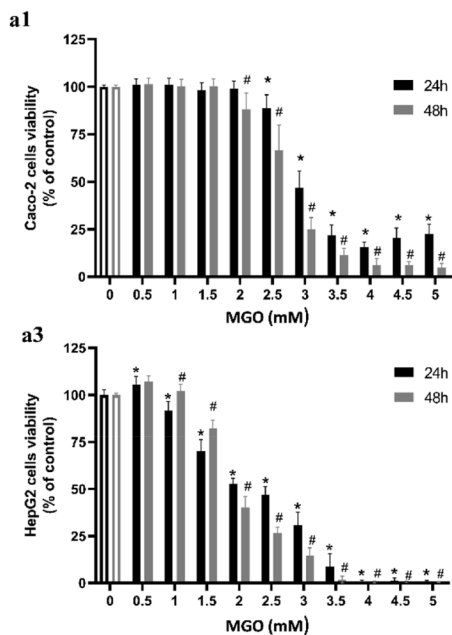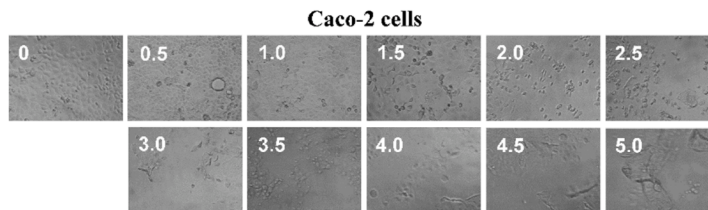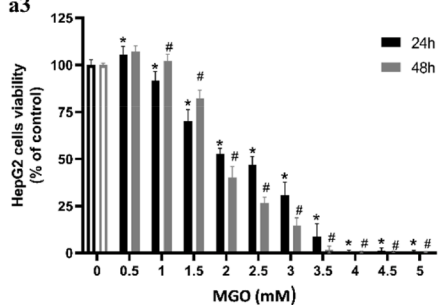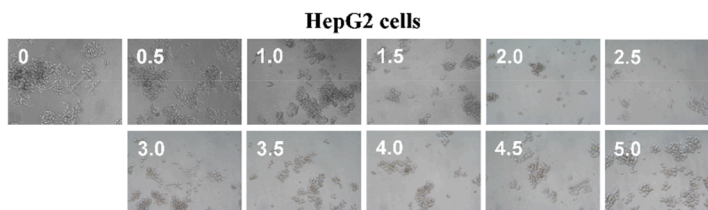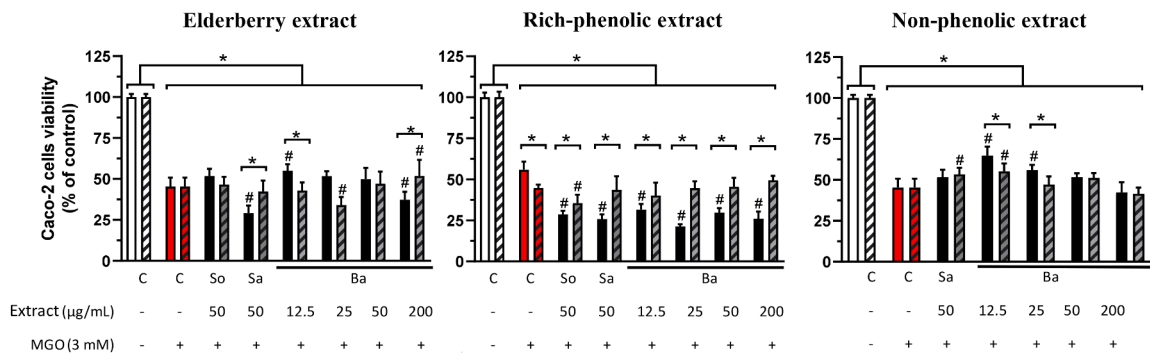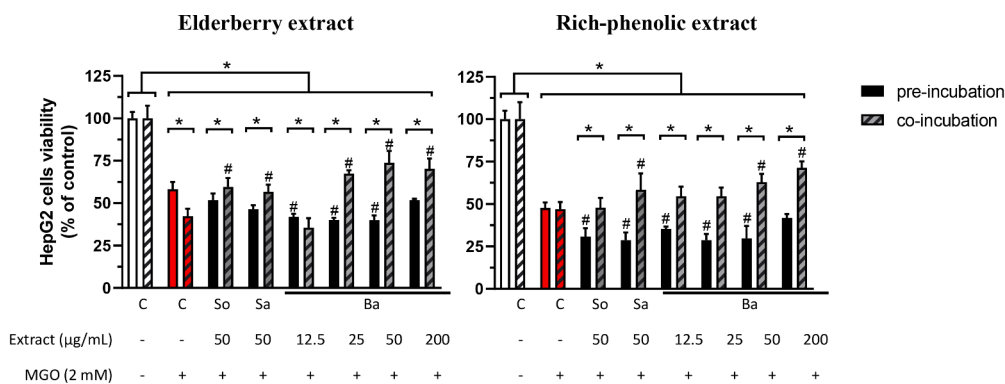
Fig. 6. Effect of methylglyoxal (MGO) and elderberry extracts using cell-models: Dose-dependent effect of exposure to MGO, for 24 h and 48 h, on Caco-2 cell viability (a1) and HepG2 cell viability (a3) and cell morphology recorded after 48 h of exposure to MGO (a2 and a4, Caco-2 and HepG2 cells, respectively), photos captured using an ocular camera (ODC-89 camera, Kern & Sohn) coupled to a microscope (amplification 100x). (Significant differences between samples and control cells ($p < 0.05$) are denoted by *and #, for 24 h and 48 h of exposure to MGO, respectively). b) Evaluation of cytoprotective effect promoted by pre- or co-incubation of Caco-2 cells with elderberry extracts [(elderberry extract (E), rich-phenolic extract (M), and non-phenolic extract (H)], from Sabugueiro (So), Sabugueira (Sa) and Bastardeira (Ba) cultivars, against 3 mM MGO. c) Evaluation of cytoprotective effect promoted by pre- and co-incubation of HepG2 cells with elderberry extracts against [(elderberry extract (E) and rich-phenolic extract (M)], from Sabugueiro (So), Sabugueira (Sa) and Bastardeira (Ba) cultivars, against 2 mM MGO. In b) and c), statistical significance ($p < 0.05$) between control cells and samples is denoted as *; the # compares extracts with the MGO control at the respective condition; and * over a square bracket compares pre- and co-incubation at the same concentration.

(Fig. 6b and c).

As shown in Fig. 6b, pre-incubation of Caco-2 cells with elderberry rich-phenolic extracts did not provide cellular protection against MGO. Pre-incubation of cells with elderberry extract and non-phenolic extract also did not offer cellular protection against MGO exposure, with the exception of 12.5 µg/mL of both Bastardeira extracts that significantly improved cell viability ($p < 0.05$, compared to MGO control). Caco-2 cells treated with rich-phenolic extract and MGO (co-incubation), on average, showed improved cell viability compared with pre-incubation condition but did not reduce MGO-induced toxicity. The same was observed for cells co-incubated with elderberry extract and MGO, in which, on average, slightly higher cell viability was obtained. Nevertheless, co-incubation of cells with elderberry non-phenolic extracts and MGO gave the same effect as pre-incubation (Fig. 6b, rightmost panel).

Results obtained for pre-incubation of HepG2 cells with elderberry extracts followed by exposure to 2 mM MGO (Fig. 6c, black bars) showed that rich-phenolic extract and elderberry extract did not offer cellular protection against MGO (2 mM). On the other hand, co-incubation of HepG2 cells with MGO and elderberry or rich-phenolic extracts was more effective than pre-incubation in reducing MGO-induced toxicity, as cell viability is significantly improved, demonstrating a protective effect against MGO (Fig. 6c, dashed grey bars). Co-incubation with elderberry rich-phenolic extract (M) reduced MGO-induced cytotoxicity, being Bastardeira the cultivar with the highest protective effect against MGO, followed by Sabugueira ($p < 0.05$, compared to MGO control), while elderberry rich-phenolic extract from Sabugueiro cultivar did not show differences from MGO control (Fig. 6c).

In Fig. 6c, HepG2 co-incubation with MGO and Bastardeira (Ba) elderberry extract at 12.5 µg/mL showed the lowest cell viability (35.46 ± 5.71 % of untreated control cells), being the only tested concentration of elderberry extract that did not show the capacity to revert MGO-induced cytotoxic effect. Increasing the concentration of Bastardeira elderberry extract from 12.5 to 25 µg/mL increased significantly ($p < 0.0001$) the cytoprotective effect against MGO-provoked injuries, giving a cell viability of 67.44 ± 1.95 % of untreated control. While 50 and 200 µg/mL promoted a cell viability higher than 70 % (Fig. 6c).

Co-incubation of HepG2 cells with rich-phenolic extract (M) from Sabugueiro and MGO did not show significant protective effect, in contrast with Sabugueira ($p = 0.0196$) and Bastardeira extracts ($p = 0.0019$) as both decreased the cytotoxicity of MGO, producing a similar protective effect. As observed, Bastardeira rich-phenolic extract showed a dose-dependent protective effect (Fig. 6c, right panel), with significant improvement of cell viability at 50 and 200 µg/mL of Ba rich-phenolic extract against 2 mM MGO, being the cell viability equal to 62.98 ± 4.81 % and 71.37 ± 3.81 %, respectively ($p < 0.0001$, compared with untreated cells control), counteracting the cytotoxicity promoted by MGO. In this way, in HepG2 cells, both extracts demonstrated a protective effect against the injuries provoked by MGO when co-incubated.

Combining the results obtained using both *in-vitro* free-cell and cell models, the polyphenols present in elderberries, when co-incubated with high doses of MGO, decrease notably MGO cytotoxicity in HepG2 cells. Due to the formation of mono- and di-adducts between MGO and phenolic compounds, mainly between cyanidin-3-glucoside and cyanidin-3-sambubioside, the major compounds present in *S. nigra* berries are able to rapidly trap MGO forming both adducts, which considerably decrease the amount of free MGO that reaches the cells and, consequently, decrease its cytotoxicity, depending firstly on the ratio between MGO and the trapping agent and then depending in its metabolism.

As far as we know, this work is the first approach that evaluated the potential cytoprotective/antiglycative effect of elderberries against the deleterious effects of MGO, using Caco-2 and HepG2 cells. However, several studies addressed the damage caused by MGO in other cell lines and the potential protective effect of bioactive compounds provided by other plant species or by isolated compounds, using different treatments, concentrations and exposure times, which make a comparison between the different studies difficult. For instance, Jiménez-Aspee et al. (2016) evaluated the cytoprotective effect of five Chilean wild raspberry (*Rubus geoides* Sm.) rich-phenolic extracts from different regions and of *Rubus idaeus* rich-phenolic extract against MGO in epithelial gastric AGS cells. AGS cells were pre-treated overnight with various concentrations of extracts (62.5, 125, 250 and 500 µg/mL), then cells were challenged for 2 h with 15 mM MGO, and cell viability was determined by MTT assay. Their results showed that the exposure of cells to MGO for 2 h significantly decreased cell viability compared to the untreated control (62.8 %). In contrast, only two samples of *R. geoides* at 500 µg/mL showed cytoprotective effect (67.8 and 64.8 % of cell viability, from San Juan and Lago Blanco, respectively). Only one sample of *R. geoides* from Las Raíces showed a significant protective effect at lower concentrations (62.5, 125 and 200 µg/mL). On the other hand, co-incubation treatment did not show significant protection against MGO (Jiménez-Aspee et al., 2016). Their findings showed that pre-treatment with *R. geoides* extracts significantly increased the levels of GSH, pointing out that the cytoprotective effect might be due to the enzymatic activity involved in the detoxification/inactivation of MGO rather than trapping MGO directly.

Phenolic compounds in peanuts also demonstrated an antiglycative potential using a BSA model and cytoprotective effect against MGO in human umbilical vein endothelial (HUVECs) cells (Park, Do, Lee, Jeong, Lim, & Kim, 2017). HUVECs cells were pre-treated for 1 h with 1, 10 and 100 µg/mL of peanut extract and then challenged for 24 h with 400 µM MGO. Park, Do, Lee, Jeong, Lim, and Kim (2017) showed that peanut extract at 100 µg/mL significantly increased cell viability compared to the MGO control, preventing MGO-induced cytotoxicity in HUVECs cells.

Concerning the use of isolated compounds, PC-12 neuron-like cells were pre-treated for 24 h with moscatilin (0.1–1 µmol/L), a bibenzyl compound present in *Dendrobium* species, and then challenged with 200 µmol/L MGO, showed a significant increase in cell viability (Lai, Liu, Liou, & Liu, 2020). Pre-treatment of rat pancreatic β-cells (RIN-m5F cells) for 1 h with Magnolol, a biphenyl compound from *Magnolia officinalis,* then exposure to 300 µM MGO for 48 h, showed significant inhibition of MGO-induced cytotoxicity (Suh, Chon, Jung, & Choi, 2017).

These studies demonstrated that pre-treatment with different extracts and concentrations in different cell lines, different concentrations of MGO and time of exposure effectively protected against MGO-induced toxicity. Our results showed that elderberry extracts displayed the cytoprotective effect by trapping MGO directly. Since the concentrations applied for the pre-treatment did not demonstrate a preventive role in protecting indirectly Caco-2 and HepG2 cells, through increasing the levels of antioxidant enzymatic defence, as GSH is essential for the detoxification system, present in the intestinal epithelium and liver, for the excretion by the efflux transporters (Satsu, 2017).

4. Conclusion

The results obtained in this work show for the first time that phenolic compounds present in elderberry have antiglycation activity by trapping MGO. Of all phenolic compounds present in elderberry extracts, the main anthocyanins in elderberries, cyanidin-3-glucoside and cyanidin-3-sambubioside, and to a lesser extent quercetin-3-glucoside and quercetin-3-rutinoside, are also able to efficiently trap MGO through the formation of mono- and di-MGO adducts. Anthocyanins present in elderberry extracts but substituted in A-ring with glucose, cyanidin-3,5-glucoside, and cyanidin-3-sambubioside-5-glucoside were not able to trap MGO under our experimental conditions. Co-incubation of cells with MGO and elderberry extracts resulted in a lower MGO cytotoxicity for HepG2 cells. The same effect was not observed for Caco-2 cells. The decrease in MGO-induced HepG2 cells toxicity can be attributed to the ability of elderberry extracts to trap MGO, an effect mainly attributed to cyanidin-3-glucoside and cyanidin-3-sambubioside, but also to cellular metabolism.

CRediT authorship contribution statement

Sandrine S. Ferreira: Formal analysis, Investigation, Writing – original draft, Writing – review & editing. **M. Rosário Domingues:** Formal analysis, Writing – review & editing, Supervision. **Cristina Barros:** Formal analysis, Investigation. **Sónia A.O. Santos:** Formal analysis, Investigation, Writing – review & editing. **Armando J.D. Silvestre:** Formal analysis, Writing – review & editing. **Amélia M. Silva:** Conceptualization, Formal analysis, Writing – original draft, Writing – review & editing, Supervision, Project administration, Funding acquisition. **Fernando M. Nunes:** Conceptualization, Formal analysis, Writing – original draft, Writing – review & editing, Supervision, Project administration, Funding acquisition.

Declaration of Competing Interest

The authors declare that they have no known competing financial interests or personal relationships that could have appeared to influence the work reported in this paper.

Appendix A. Supplementary data

Supplementary data to this article can be found online at https://doi.org/10.1016/j.fochx.2022.100468.

References

Andrea-Silva, J., Cosme, F., Ribeiro, L. F., Moreira, A. S. P., Malheiro, A. C., Coimbra, M. A., … Nunes, F. M. (2014). Origin of the pinking phenomenon of white wines. *Journal of Agricultural and Food Chemistry, 62*(24), 5651–5659.

Brüll, L. P., Heerma, W., Thomas-Oates, J., Haverkamp, J., Kovácik, V., & Kovác, P. (1997). Loss of internal 1 → 6 substituted monosaccharide residues from underivatized and per-O-methylated trisaccharides. *Journal of the American Society for Mass Spectrometry, 8*(1), 43–49.

Chen, G. (2021). Dietary N-epsilon-carboxymethyllysine as for a major glycotoxin in foods: A review. *Comprehensive Reviews in Food Science and Food Safety, 20*(5), 4931–4949.

Chen, X.-Y., Huang, I. M., Hwang, L. S., Ho, C.-T., Li, S., & Lo, C.-Y. (2014). Anthocyanins in blackcurrant effectively prevent the formation of advanced glycation end products by trapping methylglyoxal. *Journal of Functional Foods, 8*, 259–268.

Domon, B., & Costello, C. E. (1988). A systematic nomenclature for carbohydrate fragmentations in FAB-MS/MS spectra of glycoconjugates. *Glycoconjugate Journal, 5*(4), 397–409.

Fabre, N., Rustan, I., de Hoffmann, E., & Quetin-Leclercq, J. (2001). Determination of flavone, flavonol, and flavanone aglycones by negative ion liquid chromatography electrospray ion trap mass spectrometry. *Journal of the American Society for Mass Spectrometry, 12*(6), 707–715.

Fernandez-Gomez, B., Ullate, M., Picariello, G., Ferranti, P., Mesa, M. D., & del Castillo, M. D. (2015). New knowledge on the antiglycoxidative mechanism of chlorogenic acid. *Food & Function, 6*(6), 2081–2090.

Ferreira, S. S., Silva, A. M., & Nunes, F. M. (2018). *Citrus reticulata* Blanco peels as a source of antioxidant and anti-proliferative phenolic compounds. *Industrial Crops and Products, 111*, 141–148.

Ferreira, S. S., Silva, P., Silva, A. M., & Nunes, F. M. (2020). Effect of harvesting year and elderberry cultivar on the chemical composition and potential bioactivity: A three-year study. *Food Chemistry, 302*, 125366.

Gobert, J., & Glomb, M. A. (2009). Degradation of glucose: reinvestigation of reactive α-dicarbonyl compounds. *Journal of Agricultural and Food Chemistry, 57*(18), 8591–8597.

Gugliucci, A., Bastos, D. H. M., Schulze, J., & Souza, M. F. F. (2009). Caffeic and chlorogenic acids in *Ilex paraguariensis* extracts are the main inhibitors of AGE generation by methylglyoxal in model proteins. *Fitoterapia, 80*(6), 339–344.

Henning, C., Liehr, K., Girndt, M., Ulrich, C., & Glomb, M. A. (2014). Extending the spectrum of α-dicarbonyl compounds in vivo. *The Journal of Biological Chemistry, 289*(41), 28676–28688.

Huang, S. M., Chuang, H. C., Wu, C. H., & Yen, G. C. (2008). Cytoprotective effects of phenolic acids on methylglyoxal-induced apoptosis in Neuro-2A cells. *Molecular Nutrition & Food Research, 52*(8), 940–949.

Hwang, S. H., Kim, H. Y., Zuo, G., Wang, Z., Lee, J.-Y., & Lim, S. S. (2018). Anti-glycation, carbonyl trapping and anti-inflammatory activities of chrysin derivatives. *Molecules, 23*(7), 1752.

Ionescu, C.-M., Sehnal, D., Falginella, F. L., Pant, P., Pravda, L., Bouchal, T., … Koča, J. (2015). AtomicChargeCalculator: Interactive web-based calculation of atomic charges in large biomolecular complexes and drug-like molecules. *Journal of Cheminformatics, 7*(1), 50.

Jaiswal, R., Halabi, E. A., Karar, M. G. E., & Kuhnert, N. (2014). Identification and characterisation of the phenolics of *Ilex glabra* L. Gray (Aquifoliaceae) leaves by liquid chromatography tandem mass spectrometry. *Phytochemistry, 106*, 141–155.

Jiang, K., Huang, C., Jiao, R., Bai, W., Zheng, J., & Ou, S. (2019). Adducts formed during protein digestion decreased the toxicity of five carbonyl compounds against Caco-2 cells. *Journal of Hazardous Materials, 363*, 26–33.

Jiménez-Aspee, F., Theoduloz, C., Ávila, F., Thomas-Valdés, S., Mardones, C., von Baer, D., & Schmeda-Hirschmann, G. (2016). The Chilean wild raspberry (*Rubus geoides* Sm.) increases intracellular GSH content and protects against H$_2$O$_2$ and methylglyoxal-induced damage in AGS cells. *Food Chemistry, 194*, 908–919.

Lai, M. C., Liu, W. Y., Liou, S.-S., & Liu, I. M. (2020). The protective effects of moscatilin against methylglyoxal-induced neurotoxicity via the regulation of p38/JNK MAPK pathways in PC12 neuron-like cells. *Food and Chemical Toxicology, 140*, 111369.

Li, X., Zheng, T., Sang, S., & Lv, L. (2014). Quercetin inhibits advanced glycation end product formation by trapping methylglyoxal and glyoxal. *Journal of Agricultural and Food Chemistry, 62*(50), 12152–12158.

Lv, L., Shao, X., Chen, H., Ho, C.-T., & Sang, S. (2011). Genistein inhibits advanced glycation end product formation by trapping methylglyoxal. *Chemical Research in Toxicology, 24*(4), 579–586.

Ma, H., Johnson, S. L., Liu, W., DaSilva, N. A., Meschwitz, S., Dain, J. A., & Seeram, N. P. (2018). Evaluation of polyphenol anthocyanin-enriched extracts of blackberry, black raspberry, blueberry, cranberry, red raspberry, and strawberry for free radical scavenging, reactive carbonyl species trapping, anti-glycation, anti-β-amyloid aggregation, and microglial neuroprotective effects. *International Journal of Molecular Sciences, 19*(2).

Maietta, M., Colombo, R., Lavecchia, R., Sorrenti, M., Zuorro, A., & Papetti, A. (2017). Artichoke (*Cynara cardunculus* L. var. *scolymus*) waste as a natural source of carbonyl trapping and antiglycative agents. *Food Research International (Ottawa, Ont.), 100*(Pt 1), 780–790.

Mortier, W. J., Ghosh, S. K., & Shankar, S. (1986). Electronegativity-equalization method for the calculation of atomic charges in molecules. *Journal of the American Chemical Society, 108*(15), 4315–4320.

Nokin, M.-J., Durieux, F., Peixoto, P., Chiavarina, B., Peulen, O., Blomme, A., … Bellahcène, A. (2016). Methylglyoxal, a glycolysis side-product, induces Hsp90 glycation and YAP-mediated tumor growth and metastasis. *eLife, 5*, e19375.

Oliveira, J. S., de Almeida, C., de Souza, A. M. N., da Cruz, L. D., & Alfenas, R. C. G. (2021). Effect of dietary advanced glycation end-products restriction on type 2 diabetes mellitus control: A systematic review. *Nutrition Reviews, 80*(2), 294–305.

Park, S. H., Do, M. H., Lee, J. H., Jeong, M., Lim, O. K., & Kim, S. Y. (2017). Inhibitory effect of *Arachis hypogaea* (Peanut) and its phenolics against methylglyoxal-derived advanced glycation end product toxicity. *Nutrients, 9*(11), 1214.

Pitt, J. J. (2009). Principles and applications of liquid chromatography-mass spectrometry in clinical biochemistry. *The Clinical Biochemist. Reviews, 30*(1), 19–34.

Ramos, P. A. B., Moreirinha, C., Silva, S., Costa, E. M., Veiga, M., Coscueta, E., … Silvestre, A. J. D. (2019). The health-promoting potential of Salix spp. bark polar extracts: key insights on phenolic composition and in vitro bioactivity and biocompatibility. *Antioxidants, 8*(12), 609.

Sang, S., Shao, X., Bai, N., Lo, C.-Y., Yang, C. S., & Ho, C.-T. (2007). Tea polyphenol (−)-epigallocatechin-3-gallate: A new trapping agent of reactive dicarbonyl species. *Chemical Research in Toxicology, 20*(12), 1862–1870.

Satsu, H. (2017). Molecular and cellular studies on the absorption, function, and safety of food components in intestinal epithelial cells. *Bioscience, Biotechnology, and Biochemistry, 81*(3), 419–425.

Serin, Y., Akbulut, G., Uğur, H., & Yaman, M. (2021). Recent developments in *in-vitro* assessment of advanced glycation end products. *Current Opinion in Food Science, 40,* 136–143.

Shao, X., Bai, N., He, K., Ho, C.-T., Yang, C. S., & Sang, S. (2008). Apple polyphenols, phloretin and phloridzin: New trapping agents of reactive dicarbonyl species. *Chemical Research in Toxicology, 21*(10), 2042–2050.

Silván, J. M., Assar, S. H., Srey, C., Dolores del Castillo, M., & Ames, J. M. (2011). Control of the Maillard reaction by ferulic acid. *Food Chemistry, 128*(1), 208–213.

Suantawee, T., Cheng, H., & Adisakwattana, S. (2016). Protective effect of cyanidin against glucose- and methylglyoxal-induced protein glycation and oxidative DNA damage. *International Journal of Biological Macromolecules, 93*(Pt A), 814–821.

Suh, K. S., Chon, S., Jung, W.-W., & Choi, E. M. (2017). Magnolol protects pancreatic β-cells against methylglyoxal-induced cellular dysfunction. *Chemico-Biological Interactions, 277*, 101–109.

Thilavech, T., Ngamukote, S., Abeywardena, M., & Adisakwattana, S. (2015). Protective effects of cyanidin-3-rutinoside against monosaccharides-induced protein glycation and oxidation. *International Journal of Biological Macromolecules, 75*, 515–520.

Wu, C.-H., & Yen, G.-C. (2005). Inhibitory effect of naturally occurring flavonoids on the formation of advanced glycation endproducts. *Journal of Agricultural and Food Chemistry, 53*(8), 3167–3173.

Wu, C. H., Yeh, C. T., Shih, P. H., & Yen, G. C. (2010). Dietary phenolic acids attenuate multiple stages of protein glycation and high-glucose-stimulated proinflammatory IL-1beta activation by interfering with chromatin remodeling and transcription in monocytes. *Molecular Nutrition & Food Research, 54*(Suppl 2), S127–S140.

Yeh, W.-J., Hsia, S.-M., Lee, W.-H., & Wu, C.-H. (2017). Polyphenols with antiglycation activity and mechanisms of action: A review of recent findings. *Journal of Food and Drug Analysis, 25*(1), 84–92.